A&A 423, 189–197 (2004)
DOI: 10.1051/0004-6361:20047151
© ESO 2004

Astronomy & Astrophysics

Red giants in open clusters[⋆,⋆⋆]

XI. Membership, duplicity, and structure of NGC 2477

A. Eigenbrod[1], J.-C. Mermilliod[1], J. J. Clariá[2], J. Andersen[3,4], and M. Mayor[5]

[1] Laboratoire d'Astrophysique de l'École polytechnique fédérale de Lausanne, 1290 Chavannes-des-Bois, Switzerland
e-mail: Jean-Claude.Mermilliod@obs.unige.ch
[2] Observatorio Astronómico, Universidad Nacional de Córdoba, Laprida 854, 5000 Córdoba, Argentina
[3] Astronomical Observatory, NBIfAFG, Juliane Maries Vej 30, 2100 Copenhagen, Denmark
[4] Nordic Optical Telescope Scientific Association, Apartado 474, 38 700 Santa Cruz de La Palma, Spain
[5] Observatoire de Genève, 51 Ch. des Maillettes, 1290 Sauverny, Switzerland

Received 27 January 2004 / Accepted 4 May 2004

Abstract. New, accurate radial velocities and photoelectric *UBV* photometry of 83 red-giant candidates in the field of the rich, intermediate-age open cluster NGC 2477 ([Fe/H] = −0.05, age ≃ 1 Gyr) are presented and discussed. From 49 constant-velocity members we find a mean cluster velocity of $+7.32 \pm 0.13$ km s^{-1} and confirm the membership of 76 of the stars. Among the cluster members, we identify 26 definite and 1 probable spectroscopic binaries and determine orbits for 13 of these systems, with periods ranging from 40 to 4578 days. The binary frequency is thus rather high (27/76 = 36%).
The observed internal radial velocity dispersion of the cluster, as determined from the single member stars, is 0.93 km s^{-1}, corrected for the small average observational error of 0.22 km s^{-1}. Fitting King-type models to the observed stellar density distribution and velocity dispersion, and assuming a distance of 1.25 kpc, we find the core and tidal radii of NGC 2477 to be 1.8 and 8.1 pc, respectively, and estimate that the mass of cluster stars down to $V = 17$, corresponding to ∼1 $M_\odot$, is at least 5400 $M_\odot$. The substantial differential reddening of NGC 2477 requires a more detailed study before definitive isochrone fits can be made.

Key words. stars: binaries: spectroscopic – techniques: radial velocities – star: late-type – Galaxy: open clusters and associations: individual: NGC 2477

1. Introduction

Open star clusters are important test objects for models of stellar evolution and the dynamics of stellar systems. In both cases, reliable identification of single and binary cluster members is required for a critical analysis of the colour−magnitude diagram (CMD) and other data. Accurate radial velocities covering a sufficient time span provide the most stringent identification of field stars and binaries as well as the necessary kinematic data for the analysis of the dynamical structure of the cluster.

Identifying the spectroscopic binaries, especially among the cluster giants, is of special importance in such work. First, undetected orbital motion, even in systems with periods of decades, produces spurious velocity residuals and thus leads to an overestimate of the true velocity dispersion. Second, red-giant binaries are the most massive objects in open clusters, and their distribution over the cluster area indicates whether energy equipartition has occurred.

This paper, devoted to the intermediate-age open cluster NGC 2477, continues our discussion of the membership and duplicity of red giants in open clusters, based on accurate radial-velocity data (Mermilliod et al. 2003, 2001).

NGC 2477 (RA(J2000) = 7h52m.3, Dec(J2000) = −38°33′), C0750-384, is one of the richest open clusters known. As such, it provides an unusually good statistical basis for studies of stellar and dynamical evolution in open clusters. NGC 2477 was therefore given high priority in our programme. Moreover, a special effort was made to monitor the stars over long periods (3000−5000 days) in order to identify the binaries and determine their orbits as far as possible. Our mean radial velocities are sufficiently accurate to not only securely identify cluster members and binary stars, but also to resolve the internal velocity dispersion, making NGC 2477 one of the few open clusters in which this has been achieved.

⋆ Based on observations collected with the Danish 1.54-m and ESO 1-m telescopes at the European Southern Observatory, La Silla, Chile, and with the University of Toronto 0.6-m telescope at Las Campanas Observatory, Chile.

⋆⋆ Full Tables 1 and 2 are only available in electronic form at the CDS via anonymous ftp to
cdsarc.u-strasbg.fr (130.79.128.5) or via
http://cdsweb.u-strasbg.fr/cgi-bin/qcat?J/A+A/423/189

Article published by EDP Sciences and available at http://www.aanda.org or http://dx.doi.org/10.1051/0004-6361:20047151

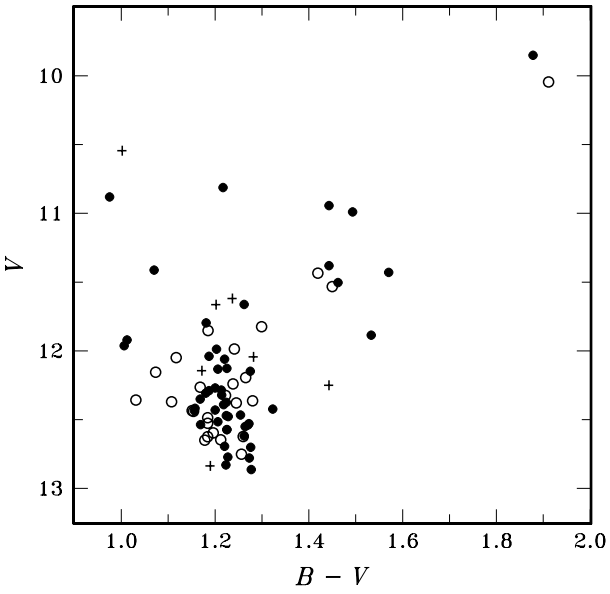

Fig. 1. CMD of the observed RGB candidates in NGC 2477. *Dots*: single members; *circles*: binary members; *plusses*: non-members.

As a complement to our radial-velocity survey, we also obtained photoelectric *UBV* photometry of all the red-giant candidates in NGC 2477. More recently, extensive CCD data of the cluster field have been obtained by Kassis et al. (1997) and Momany et al. (2001), which we use to study the radial structure of the cluster, in extension of the preliminary analysis by Raboud & Mermilliod (1994).

2. Observations

2.1. Sample definition

83 potential members of the red-giant branch (RGB) of NGC 2477 were selected from the combined photoelectric and photographic *BV* photometry of Hartwick et al. (1972) and Hartwick & Hesser (1974), the most extensive CMD available when the programme was started. Candidates were selected to have $0.9 < B - V < 2.0$ and $9.75 < V < 13.0$, the blue limit in $B - V$ being set so as to include giant spectroscopic binaries with main-sequence companions. The observed sample of stars is shown in the CMD of NGC 2477 in Fig. 1.

2.2. Radial-velocity observations

The radial-velocity observations were made with the photoelectric scanner Coravel (Baranne et al. 1979; Mayor 1985) on the Danish 1.54-m telescope at ESO, La Silla, Chile, during several observing runs from February 1983 through April 1997. The radial velocities are on the system defined by Udry et al. (1999), calibrated with high-precision data from the ELODIE spectrograph (Baranne et al. 1996). A total of 704 observations were obtained of the 83 programme stars, with a median number of 5 observations per star. Constant-velocity cluster members have a minimum of 4 observations each, binaries up to 26 observations in order to cover their orbits.

2.3. Photometric observations

Most of our *UBV* observations were made with the ESO 1-m telescope at La Silla in March 1988. A dry-ice cooled RCA 31034 (Quantacon) Ga-As photomultiplier was used with pulse-counting equipment and standard *UBV* filters. Mean extinction coefficients for La Silla were used, and 12−18 standard stars from the lists of Cousins (1973, 1974) and Graham (1982) were observed nightly to transform to the standard *UBV* system. The average external mean errors are below 0.014 mag for both V, $B - V$, and $U - B$.

Additional photometry was obtained during three nights of excellent quality in February 1987 with the University of Toronto 61-cm telescope at Las Campanas Observatory (LCO) in Chile, using a single-channel photometer with an EMI 9658 photomultiplier. The same standards were used as for the La Silla observations, and mean extinction coefficients for LCO were also employed. The average external mean errors of the LCO photometry are below 0.017 mag.

Comparison of our new photoelectric photometry with that of Hartwick et al. (1972) shows very good agreement for the 33 stars in common: $\Delta V = -0.03 \pm 0.02$, $\Delta(B - V) = -0.01 \pm 0.01$, and $\Delta(U - B) = 0.04 \pm 0.04$ (rms). Comparison with the photographic data shows small zero-point differences in V and a somewhat larger scatter, as expected (73 stars in common): $\Delta V = 0.11 \pm 0.06$ and $\Delta(B - V) = -0.05 \pm 0.08$ (rms).

3. Results

Our new radial velocities and *UBV* photometry of the red giants in NGC 2477 are given in Table 1, separately for members and non-members. The numbering system is adapted from the studies of Hartwick et al. (1972) and Hartwick & Hesser (1974), as indicated in the first three columns. The following columns list J2000 coordinates for the stars from Momany et al. (2001); the new V, $(B - V)$, and $(U - B)$ data and the number of photometric measurements N_p; the mean radial velocity, its mean error σ (km s^{-1}), the number of radial-velocity observations N_v, and the interval ΔT (days) spanned by the observations. Finally, $P(\chi^2)$ is the probability that the velocity is constant, given the known error of the individual observations (typically 0.5 km s^{-1}), and $P(RV)$ is the membership probability computed from the radial velocities (see Sect. 3.2 below). Individual radial velocities are listed in Table 2. Tables 1 and 2 are available only in electronic form. The first five lines are given as an illustration of table format and content.

$P(\chi^2) < 0.01$ and $P(RV) < 0.01$ are taken as the criteria for certain velocity variability (i.e., duplicity) and non-membership, respectively. Remarks classify the binaries (SB: spectroscopic binary without an orbital solution; SB?: probable binary; SBO: orbital solution given in Table 3). The photometry for star 7012 is from Kassis et al. (1997).

3.1. Cluster mean velocity and velocity dispersion

Based on the 49 constant-velocity cluster members in Table 1, the cluster mean radial velocity is $+7.33 \pm 0.14$ km s^{-1} with a standard deviation of 0.96 km s^{-1}. Friel et al. (2002) found a

Table 1. *UBV* photometry and radial velocities for the red giants in NGC 2477. HHM numbers refer to Hartwick et al. (1972), HH numbers to Hartwick & Hesser (1974).

No.	HHM	HH	RA (2000)	Dec	V	$B-V$	$U-B$	N_p	V_r [km s^{-1}]	σ [km s^{-1}]	N_v	ΔT [d]	$P(\chi^2)$	$P(RV)$	Rem
Members															
1008	1008		7 52 18.914	−38 31 36.35	12.358	1.031	0.610	2	+7.77	0.55	19	5171	0.000	0.687	SB
1014	1014		7 52 20.684	−38 31 11.80	12.351	1.168	0.810	2	+8.30	0.23	5	4785	0.750	0.326	
1025	1025		7 52 17.101	−38 30 08.57	12.435	1.151	0.781	2	+6.72	0.13	21	4708	0.000	0.540	SBO
1044	1044		7 52 26.637	−38 29 45.18	11.825	1.299	1.058	2	+7.46	0.13	15	5171	0.000	0.886	SBO
1069	1069		7 52 18.891	−38 28 22.21	9.851	1.878	2.251	2	+7.42	0.16	5	4697	0.531	0.919	

Table 2. Individual radial velocities.

No	HJD	V_r	σ
1008	2 445 389.613	1.07	1.17
1008	2 445 762.654	1.70	0.61
1008	2 446 466.606	3.55	0.68
1008	2 446 524.574	4.86	0.58
1008	2 446 816.694	5.75	0.46

mean velocity of +7 km s^{-1} from 28 stars, in excellent agreement with the earlier result by Friel & Janes (1993) and with our new determination. The zero-point and standard deviation (4 km s^{-1}) of the velocities by Friel et al. (2002) are in fact better than they estimate, although still larger than we find from our much more accurate data.

Assuming a Gaussian distribution of both the stellar velocities and their observational errors, we can correct the observed velocity dispersion for the contribution of the observational errors, which average 0.22 km s^{-1} (Trumpler & Weaver 1962). We find a true radial-velocity dispersion of 0.93 km s^{-1} for the single red giants in NGC 2477, a value comparable to, e.g. NGC 2099 (0.92 km s^{-1}; Mermilliod et al. 1995) and IC 4651 (0.74 km s^{-1}; Meibom et al. 2002). We later use this value to study the structure of NGC 2477 in more detail.

3.2. Membership on the RGB

Assuming again a Gaussian distribution of radial velocities and their errors for the cluster stars, we can compute individual membership probabilities $P(RV)$ for all stars as described in more detail by Nordström et al. (1997). The results are given in Table 1. The standard criterion for definite non-membership, $P(RV) < 0.010$, identifies the 7 stars 2351, 3501, 5043, 6340, 7311, 7354, and #7501 as definite non-members. The stars 6062 and 8216 also have membership probabilities below 1%, but both are binaries and their mean velocities might still be uncertain and/or affected by a third component, so we retain them as likely members, consistent with their location in the CMD.

3.3. Spectroscopic binaries on the RGB

Using the criterion $P(\chi^2) < 0.01$, we find 27 spectroscopic binaries, all among the cluster members and all single-lined. 13 orbital solutions have been derived so far; the orbital elements are given in Table 3, and the radial-velocity curves are shown in Figs. 2 and 3. The orbit of star 6251 is still preliminary because the orbital cycle is not yet adequately covered. For the remaining systems, the number and/or time span (∼14 yr) of the observations remain inadequate to determine the period and other orbital elements. The frequency of spectroscopic binaries in NGC 2477 is 36% (27/76), somewhat higher than the overall average of 23% for cluster giants as found by Mermilliod & Mayor (1992).

The orbital periods of stars 1025 (42 days) and 8017 (60 days) are quite short for red giant systems. Mayor & Mermilliod (1984) found red giant binaries to have significant orbital eccentricities above a limiting period of 120 days, and these two orbits are indeed very nearly circular. The period-eccentricity diagram of NGC 2477 (Fig. 4) shows a clear transition from circular to elliptical orbits near $P = 100$ days.

The 42-day period of star 1025 is the shortest of any giant binary orbit determined in this programme. Indeed, this value corresponds to the shortest period that a 2 $M_\odot$ star can have at the tip of the red giant branch (RGB) without experiencing Roche-lobe overflow at its maximum radius. Evolutionary models show that the stellar radius at the tip of the RGB is near a minimum for 2 $M_\odot$ stars (just above the mass limit for the helium flash to occur), which explains why the minimum period is found in a cluster such as NGC 2477 where the red giants have just this mass (see Sect. 4).

3.4. Radial-velocity profile and cluster rotation

The distribution of the radial velocities of the red giants as a function of their distances R to the cluster center is shown in Fig. 5. There is a hint of a lower velocity dispersion at the very centre and possibly in the outermost parts, but the number of stars is insufficient to allow a statistically significant conclusion.

The radial velocities of the individual stars have also been plotted as a function of their position angles relative to the cluster centre (Fig. 6). A net rotation of the cluster would cause the

Table 3. Orbital parameters.

No.	Period	T	e	γ	ω	K	f(m)	$a \sin i$	σ	$n_{\rm obs}$
	[d]	[HJD]		[km s^{-1}]	[deg]	[km s^{-1}]	[$M_\odot$]	[Gm]	[km s^{-1}]	
1025	41.5540	49 991.8	0.040	6.72	240.	11.75	0.00698	6.71	0.50	21
	0.0044	2.4	0.016	0.13	20.	0.21	0.00039	0.13		
1044	3108.	47 747.	0.074	7.46	157.	3.22	0.0107	137.	0.47	15
	52.	358.	0.060	0.13	42.	0.20	0.0023	11.		
2064	4578.	48 031.	0.273	6.14	222.5	5.78	0.0819	350.	0.29	18
	76.	45.	0.022	0.09	3.9	0.13	0.0084	16.		
2204	1318.9	49 157.3	0.581	7.62	244.8	19.47	0.545	287.	0.69	18
	5.0	10.0	0.012	0.18	1.6	0.41	0.053	10.		
3003	1782.4	48 059.	0.355	7.49	15.3	11.13	0.209	255.2	0.54	23
	4.9	16.	0.015	0.13	3.5	0.24	0.018	7.7		
3176	276.74	49 964.8	0.153	7.01	28.7	7.74	0.01286	29.10	0.44	26
	0.17	5.3	0.016	0.09	6.7	0.13	0.00073	0.56		
4137	372.367	49 465.9	0.374	9.04	142.6	14.56	0.0952	69.14	0.32	26
	0.069	1.0	0.005	0.11	1.5	0.10	0.0025	0.63		
5073	326.10	50 024.4	0.579	6.13	169.0	14.66	0.0579	53.6	0.50	21
	0.12	1.1	0.008	0.12	1.4	0.26	0.0043	1.3		
6020	226.20	49 686.4	0.367	8.55	313.2	9.33	0.0154	27.00	0.57	22
	0.11	2.1	0.019	0.13	3.7	0.22	0.0015	0.89		
6062	482.3	49 338.	0.103	10.16	243.	6.21	0.0118	41.0	0.73	19
	1.1	36.	0.053	0.21	26.	0.32	0.0021	2.5		
6251	412.6	49 637.	0.117	7.40	110.	1.92	0.00030	10.8	0.58	10
	3.2	90.	0.146	0.20	81.	0.28	0.00015	1.8		
8017	60.3169	49 866.26	0.000	8.33	360.	21.74	0.0643	18.03	0.79	21
	0.0083	0.38	0.014	0.19	313.	0.25	0.0023	0.21		
8018	140.149	49 780.9	0.274	6.28	349.7	6.77	0.00401	12.54	0.26	15
	0.044	1.5	0.018	0.08	3.8	0.12	0.00029	0.30		

points to scatter around a sine curve in this diagram. No evidence is seen for any such sine curve with an amplitude larger than 0.5 km s^{-1}, so no net rotation of NGC 2477 is discernible.

We note that no significant difference between single and binary stars is seen in Figs. 5 and 6, in line with the lack of significant evidence for mass segregation in NGC 2477 (Sect. 5.3 and Fig. 10).

3.5. Cluster radial-velocity distribution

Models describing the spatial structure of a cluster require an expression for the velocity distribution. We assume here that it is given by the approximation to the steady-state solution of the Fokker-Planck equation formulated by King (1966). Evaluated at the center of the cluster (i.e. at $r = 0$), this results in the following lowered Gaussian distribution:

$$f_{\rm RG}(v) = k_{\rm RG}\left[\exp\left(-\frac{v^2}{2\sigma_{\rm RG}^2}\right) - \exp\left(-\frac{v_{\rm e}^2}{2\sigma_{\rm RG}^2}\right)\right] \quad (1)$$

where v is the stellar radial velocity in the cluster rest frame; $v_{\rm e}$ is the escape velocity (at $r = 0$), $\sigma_{\rm RG}$ is the velocity dispersion (before lowering), and $k_{\rm RG}$ is the central density of giant stars. $v_{\rm e}$ can be estimated as follows (Chandrasekhar 1957):

$$v_{\rm e} \simeq 2\sqrt{3}\,\sigma_{\rm RG} = 3.22 \text{ km s}^{-1}. \quad (2)$$

We then compute the corresponding cumulative distribution of radial velocities $C(v)$,

$$C(v) = \frac{\int_{-v_{\rm e}}^{v} f(0,v')\mathrm{d}v'}{\int_{-v_{\rm e}}^{v_{\rm e}} f(0,v')\mathrm{d}v'} \quad (3)$$

and compare it to the observed distribution $C_{\rm obs}$ as derived from the 49 single stars plus 12 binaries with orbital solutions (Fig. 7).

As seen, the computed curve fits the observed distribution very well. To obtain a quantitative estimate of the goodness-of-fit, we apply a χ^2 test, binning the observed velocities in 12 intervals and comparing the predicted and observed

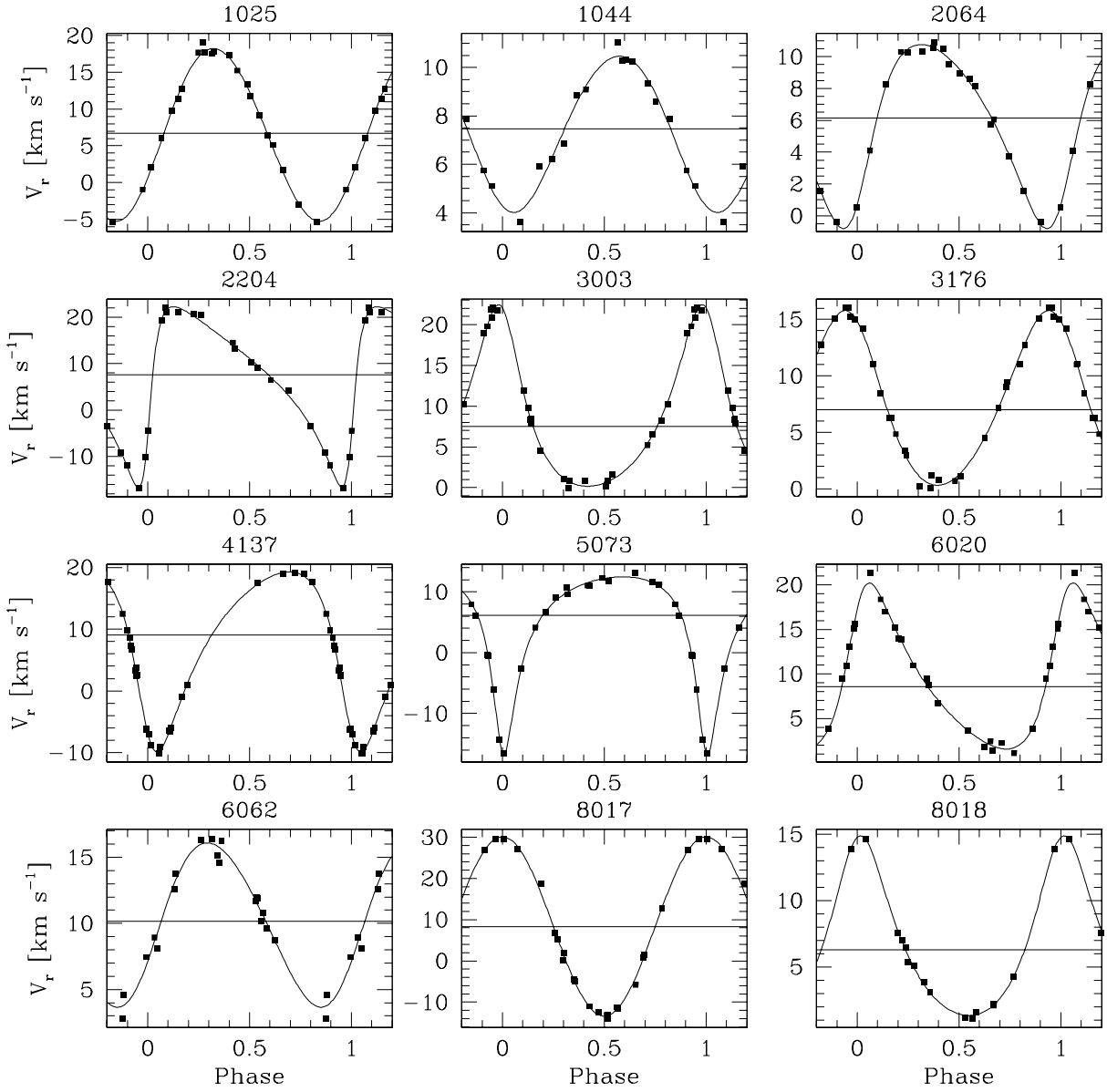

Fig. 2. Radial-velocity curves for twelve spectroscopic binaries.

numbers of velocities in each bin. The resulting value of χ^2 is 1.67 for 11 degrees of freedom, corresponding to a probability $Q(\chi^2|\nu)$ of 0.999; the lowered Gaussian is thus an excellent approximation to the observed cumulative radial-velocity distribution.

4. General properties of NGC 2477

For the discussion of the structure and evolution of NGC 2477, a summary of its overall properties will be useful. These include the reddening, distance, metal abundance, age, membership of unevolved stars, and the masses of member stars at key points of the cluster sequence. We discuss each of these in turn in this section, making use of the *BV* CMD of NGC 2477 by Momany et al. (2001) because of the large field covered ($34' \times 33'$), more than four times that observed in *BVI* by Kassis et al. (1997).

As shown already by Hartwick et al. (1972) and Hartwick & Hesser (1974), NGC 2477 is affected by differential reddening ranging from $E(B-V) \simeq 0.2$ to 0.4 mag, with a mean value near 0.30 mag (confirmed by Kassis et al. 1997 and Friel et al. 2002). This fact considerably complicates all discussions of the properties of NGC 2477, but can be handled as shown in the following.

The distance modulus of NGC 2477 was determined by Hartwick et al. (1972) to $(m-M)_0 = 10.6 \pm 0.2$ mag, while Kassis et al. (1997) found it to be 10.5 ± 0.3 mag, corresponding to a distance of 1.25 ± 0.2 kpc. We adopt the latter value in the following.

The most recent spectroscopic determination of metallicity of NGC 2477 is by Friel et al. (2002). Retaining the 21 single radial-velocity members in common with our Table 1, we find a mean [Fe/H] $= -0.14$ dex, with a standard deviation (1σ) of 0.10 dex. We note that Gratton (2000) found a

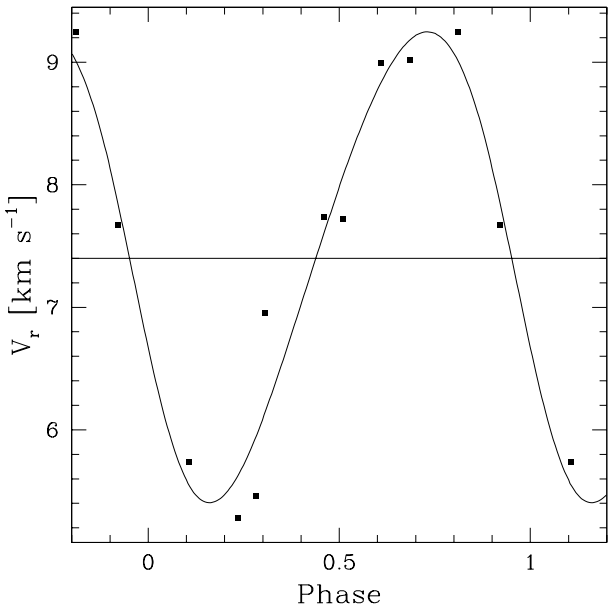

Fig. 3. Preliminary orbit of star 6251.

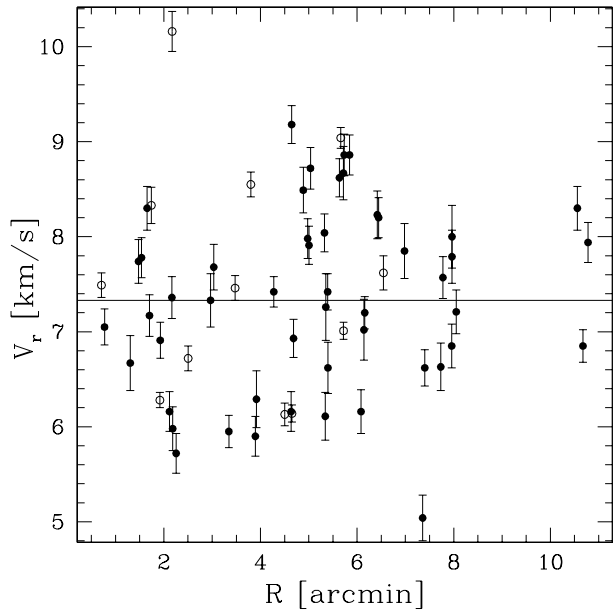

Fig. 5. Radial velocity of the red giants as a function of their distance to the cluster center. There is a hint of a decrease with increasing R, but the center seems to be depleted of red giants. Open circles: spectroscopic binaries with orbital elements, filled circles: single red giants.

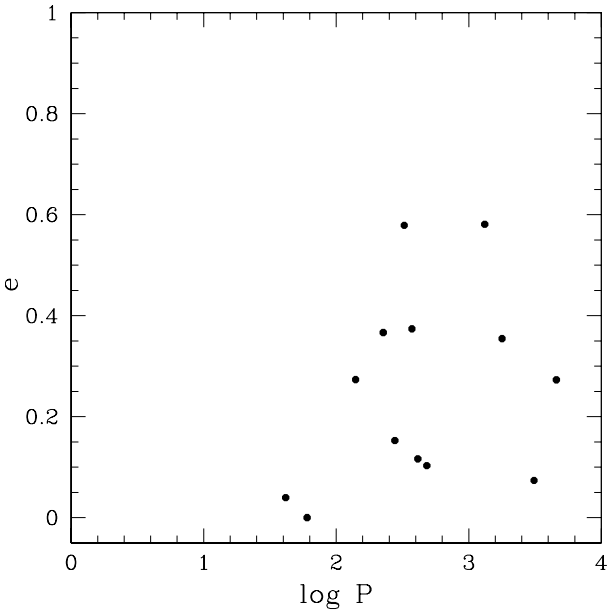

Fig. 4. Period – eccentricity diagram for NGC 2477.

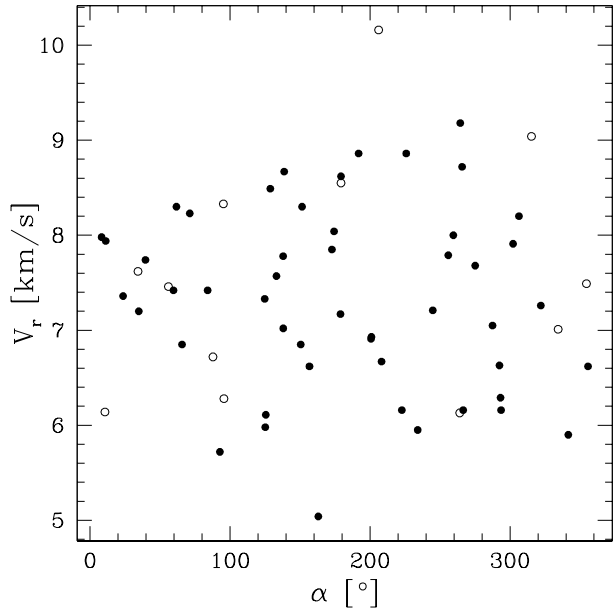

Fig. 6. Radial velocity plotted in function of the position angle α. No rotation of the cluster is evident. Symbols as in Fig. 5.

correction of −0.10 dex to the earlier results of Friel & Janes (1993) and gave [Fe/H] = 0.00 for NGC 2477. Given the overall uncertainties, it seems safe to assume a solar composition (Z = 0.019) for NGC 2477.

In order to estimate the age of NGC 2477 and the individual masses of the selected member stars, we have fit the Momany et al. (2001) BV CMD with isochrones from Girardi et al. (2000) for Z = 0.019 as the closest match to the metallicity of NGC 2477. Given the presence of variable reddening in NGC 2477, we have retained the value $(m - M)_0$ = 10.5 and fit the blue edge, red edge, and middle of the observed main sequence for the minimum, maximum, and average reddening ($E(B - V)$ = 0.22, 0.40, and 0.30), respectively, adopting $R = A_V/E(B - V)$ = 3.2. As seen in Fig. 8, these curves account well for the observed distribution of the stars on the main sequence as well as on the giant branch for a single distance, metallicity, and age (1.0 Gyr), consistent with Kassis et al. (1997) and Friel et al. (2002), varying only the reddening within the observed range. More precise reddening data will be needed to derive a substantially more reliable age than our present estimate.

In order to study the structure of NGC 2477, we need to consider the main-sequence stars as well as the red giants. Because no radial velocities are available for the

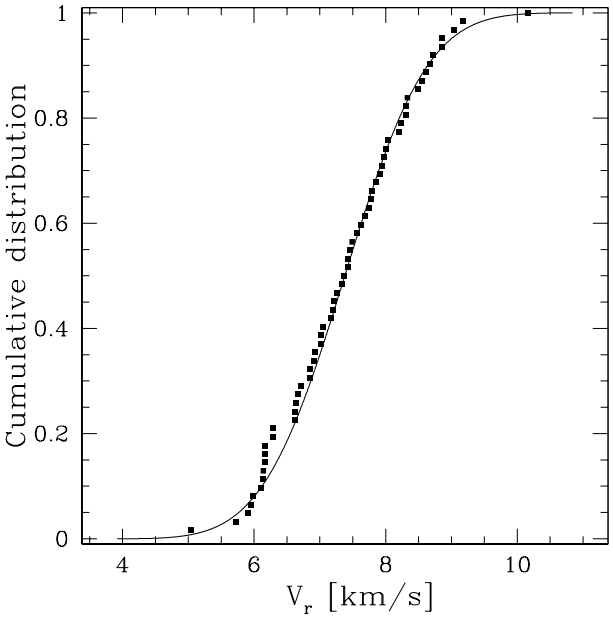

Fig. 7. Comparison of the observed (squares) and computed (line) cumulative radial-velocity distribution function, assuming a lowered Gaussian distribution.

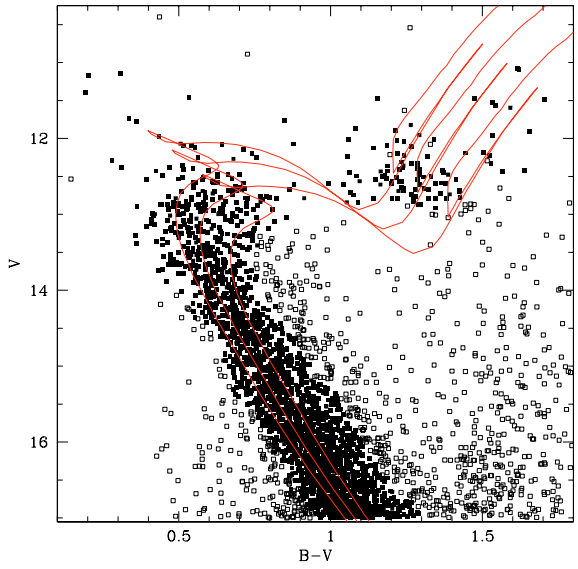

Fig. 8. *BV* CMD of NGC 2477 from Momany et al. (2001) for $V \leq 17$. The curve shows the fitted 1-Gyr isochrones for the minimum, average, and maximum reddening observed in the cluster (see text). Stars assumed to be members from their proximity to the isochrone are plotted as filled squares; empty squares denote stars assumed to be non-members.

main-sequence stars, we selected candidates on purely photometric grounds from the wide-field *BV* CCD photometry by Momany et al. (2001), which should cover most of even this large cluster. Our selection is shown in Fig. 8, restricted to stars with $V \leq 17$ because field stars overwhelm the cluster sequence at fainter magnitudes. An improved background star identification or subtraction would require observations of the radial velocities of the individual stars, such as we suggest in Sect. 7, or observations of an even larger field around NGC 2477 than that of the study by Momany et al. 2001).

Model masses on the isochrone for the average reddening value are 2.1 $M_\odot$ in the giant clump, 2.0 $M_\odot$ at the red end of the turnoff and 1.75 $M_\odot$ at its bluest point. Masses down the main sequence are then 1.6, 1.3, 1.1. and 1.0 $M_\odot$ at V = 14, 15, 16, and 17, respectively.

5. The structure of NGC 2477

5.1. Dynamical models

To describe the structure of NGC 2477, we use the King (1966) models as extended by Tinsley & King (1976) to include a mixture of different stellar types (i.e. masses). Thus, the mass density at each point in the cluster is the sum of the contributions by the individual groups or mass bins. The density distribution is found by solving Poisson's equation, so that the density and velocity distributions are mutually consistent.

The velocity distribution $f_i(r, v)$ of the ith group is described by a lowered Gaussian:

$$f_i(r,v) = k_i \exp\left(\frac{V_0}{\sigma_i^2}\right)\left[\exp\left(-\frac{v^2}{2\sigma_i^2} - \frac{V(r)}{\sigma_i^2}\right) - 1\right] \quad (4)$$

where r is the distance to the center of the cluster and v is the stellar velocity in the cluster rest frame. The gravitational potential $V(r)$ of the cluster is set to V_0 at the centre and zero at the surface of the cluster. The factors k_i are taken to be proportional (by a constant α) to the observed number of stars of the ith group multiplied by the average mass m_i of the stars of the group. The velocity dispersions σ_i (before lowering) correspond to equipartition (i.e. $m_i\sigma_i^2 = m_j\sigma_j^2$). Since the velocity dispersion of the red giants is already known, as are the m_i's, the velocity dispersions of the other groups are easily computed.

As in the King (1966) models, the density of each group is found, at any value of the potential, by integrating over the velocity distribution; we can then compute the surface density $F(r)$ for the model, projected on the plane of the sky. For comparison, the observed surface density $F_{\rm obs}$ is computed for N_r by dividing the total stellar mass M_j in successive concentric rings by their areas, A_j. From Poisson statistics, the uncertainty is $\delta F_{\rm obs} = \sqrt{M_j}/A_j$.

The adjustable parameters in fitting a model to NGC 2477 are now the central value of the potential, V_0, and the constant α, and we determine them so as to minimise the quantity:

$$\sum_{j=1}^{N_r} \frac{\left(F_{{\rm obs},j} - F(r_j)\right)^2}{\delta F_{{\rm obs},j}} \quad (5)$$

where r_j is the mean radius of the jth ring.

The resulting parameters are $V_0 = -5.25$ km^2 s^{-2}, $\alpha = 1515$ the tidal radius $r_{\rm t} = 8.10$ pc (=22.7′) and the radius $r_{\rm c} = 1.80$ pc (=4.9′), similar to the empirical "core radius" defined by King (1962), while the fit itself is shown in Fig. 9. The model has a total mass of about 5400 $M_\odot$ out to the tidal radius $r_{\rm t}$, which is a lower limit because we only consider stars with $V \leq 17$ ($M \geq 1\ M_\odot$).

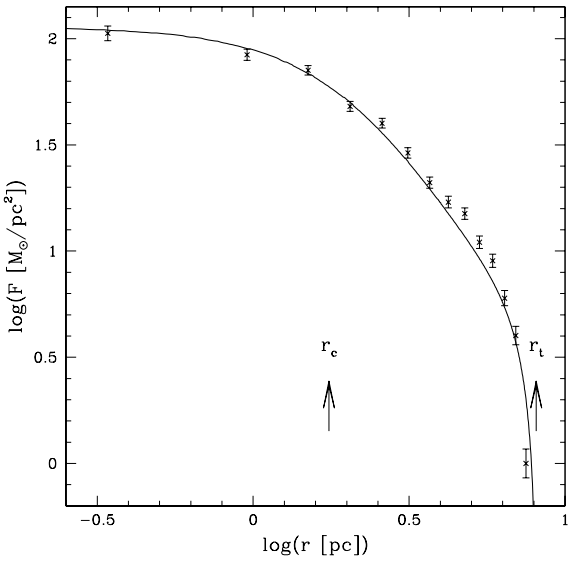

Fig. 9. The radial density profile of NGC 2477. The line shows the fitted model, and the core and tidal radii r_c and r_t are marked.

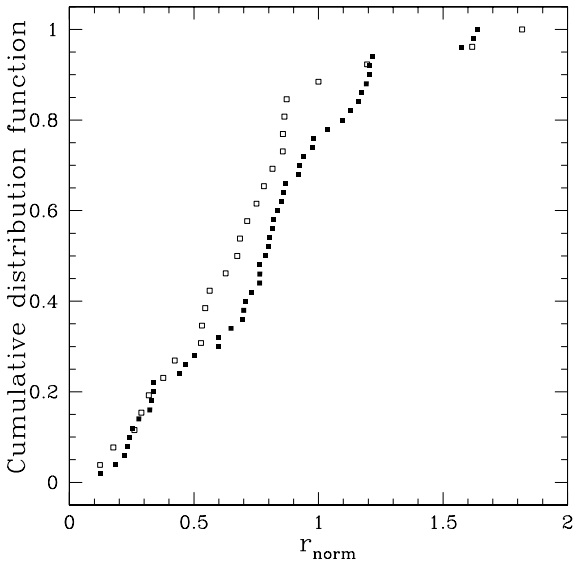

Fig. 10. The cumulative radial surface distributions of binary (open squares) and single red giants (filled squares).

Note that our value of r_t is close to half of the diagonal of the field observed by Momany et al. (2001). However, the shape of the curve in Fig. 9 is well determined from the inner parts of the field, so we believe that our result for r_t should not be significantly influenced by truncation effects.

5.2. Virial mass of NGC 2477

Assuming velocity isotropy, the virial mass of the cluster is:

$$M_C = \frac{6\,\bar{r}\,\overline{v_r^2}}{G}. \quad (6)$$

The harmonic radius $\bar{r}$ is 3.8 pc in the present case (Schwarzschild 1954). Since the velocity distribution of the red giants is known and very nearly Gaussian (i.e. $\overline{v_r^2} \simeq \sigma_v^2$), we find a lower limit to the cluster mass of about 5300 $M_\odot$, in good agreement with the previous result.

5.3. Surface distribution of the red-giant binaries

Following Raboud & Mermilliod (1994), we compute the cumulative distribution of the radial distances r from the cluster centre and define R_{80} as the radius containing 80% of the stars; we find $R_{80} = 6.55'$. Normalising the radial distances to R_{80} ($r_{norm} = r/R_{80}$), we show the cumulative distributions of single and binary red giants in Fig. 10 to illustrate the degree of central concentration of these two mass groups.

While the binaries appear slightly more centrally concentrated than the single stars, a Kolmogorov-Smirnov test yields a probability of only 51.1% that the two distributions are really different. Thus, the concentration of binaries towards the center is not statistically significant, in agreement with the earlier results of Raboud & Mermilliod (1994) for open clusters of log (age) < 9, but strikingly differs from the case of NGC 1817 which has a similar age, 39 red-giant members, and a strong concentration of spectroscopic binaries towards the centre (Mermilliod et al. 2003).

6. The RGB of NGC 2477 in the colour–magnitude diagram

With 76 red giants with well-established membership and duplicity credentials, NGC 2477 should allow a detailed study of RGB morphology in the CMD. This task is, however, rendered more difficult by the substantial reddening variations over the cluster, which seem not to follow any well-defined pattern (Hartwick et al. 1972).

When plotted first with a constant $E(B-V) = 0.22$ mag, the stars scatter considerably in the CMD (Fig. 11a). Correcting the individual stars for reddening using the $(U-B, B-V)$ diagram improves the situation considerably (Fig. 11b), although no really well-defined sequence emerges. Finally, correcting for the mean reddening at different positions in the cluster gives an even better result, as can seen in Fig. 11c.

The previously fitted isochrone from Girardi et al. (2000) reproduces the observed distribution of the red giants in NGC 2477 fairly well; most are located in the blue part of the loop, where the models predict the slower evolution. In this respect, the distribution of the red giants in NGC 2477 is quite similar to that found in NGC 1817 by Mermilliod et al. (2003).

A number of well-established radial-velocity members seem to fall in the Hertzsprung gap, although they are not (yet) detected as binaries. These stars might be affected by image crowding in the photometry, or they might be binaries of very long period and low velocity amplitude.

7. Conclusions

Our precise, long-term Coravel radial-velocity observations of 83 red giants in the field of the rich open cluster NGC 2477 yield a mean velocity of $+7.33 \pm 0.14$ km s^{-1} and identify 76 stars as certain cluster members. We also discover 26 certain and 1 probable spectroscopic binaries among the cluster members; 13 orbits have been determined so far. Combining these and other available data, we confirm

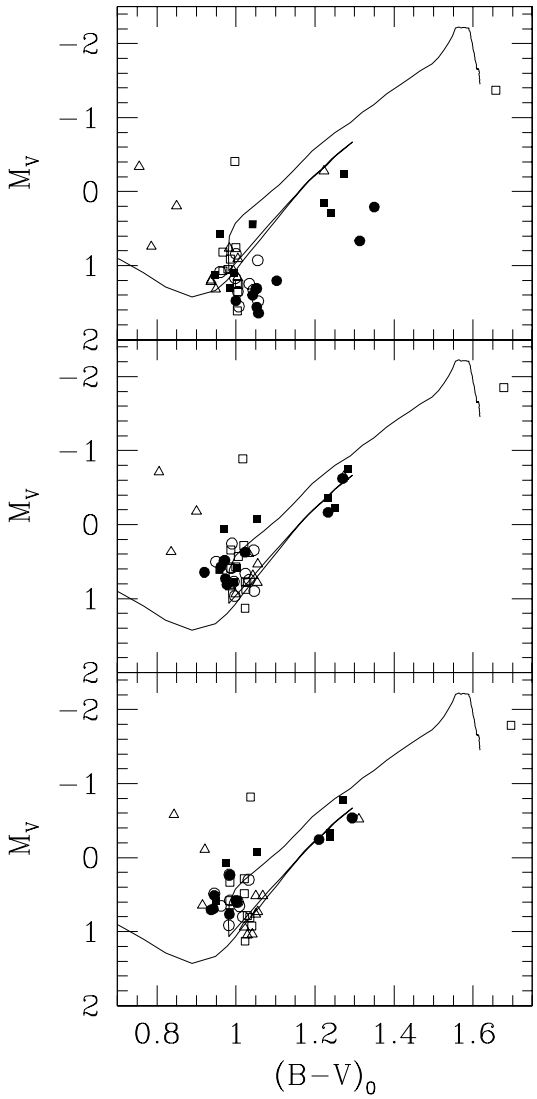

Fig. 11. The RGB of NGC 2477 in the *BV* CMD. *Top*: uniform reddening; *middle*: individual reddening corrections; and *bottom*: regional reddening means. Stars are labelled by value of $E(B-V)$ as follows: *triangles*: 0–0.178, *open squares*: 0.178–0.203, *filled squares*: 0.203–0.225, *circles*: 0.225–0.265, and *dots*: 0.265–0.359. The isochrone is the same as in Fig. 8.

that NGC 2477 has a metal abundance of [Fe/H] = −0.14, a distance of 1.25 kpc, and intermediate age (∼1 Gyr). Substantial reddening variations over the cluster complicate the analysis, however.

The true internal velocity dispersion of NGC 2477 is 0.93 km s^{-1}, much larger than the errors of the mean stellar velocities, 0.22 km s^{-1}. Together with the projected radial density profile, this allows us to construct a King-type model of the cluster and estimate a total mass of 5400 $M_\odot$ in stars brighter than $V = 17$ (∼1 $M_\odot$), very close to the 5300 $M_\odot$ derived from the virial theorem. The core and tidal radii of NGC 2477 are 1.8 and 8.1 pc, respectively.

The red-giant binaries in NGC 2477 are not significantly more centrally concentrated than the single giants, suggesting that relaxation and energy equipartition have not yet been reached. The new generation of multi-object spectrographs, such as GIRAFFE at the ESO VLT, will make it easy to observe solar-type stars in NGC 2477 with good accuracy. A survey comprising at least 5 velocities per star over a few years would yield data similar to those presented here, but for stars of half the mass, and would enable us to verify the hypothesis of equipartition in unprecedented detail.

Acknowledgements. This project was made possible by substantial grants of ESO and Danish observing time and travel support, and by observations contributed by other colleagues from Geneva and Copenhagen. We are also grateful to Dr. Emilio Lapasset who carried on the photometric observations at Las Campanas. J.A. thanks the Danish Natural Science Research Council for financial support. J.J.C. acknowledges the financial support of the CONICET.

References

Baranne, A., Mayor, M., & Poncet, J.-L. 1979, Vistas Astron., 23, 279
Baranne, A., Queloz, D., & Mayor, M., et al. 1996, A&AS, 119, 373
Chandrasekhar, S. 1957, Principles of stellar dynamics (New York: Dover Publications, Inc.)
Cousins, A. W. J. 1973, Mem. RAS, 77, 223
Cousins, A. W. J. 1974, MNASSA, 33, 149
Friel, E. D., & Janes, K. A. 1993, A&A, 267, 75
Friel, E. D., Janes, K. A., Tavarez, M., et al. 2002, AJ, 124, 2693
Girardi, L., Bressan, A., Bertelli, G., et al. 2000, A&AS, 141, 371
Graham, J. A. 1982, PASP, 92, 244
Gratton, R. G. 2000, in Stellar clusters and associations: Convection, rotation, and dynamos, ed. R. Pallavicini, G. Micela, & S. Sciortino, ASPC, 198, 225
Hartwick, F. D. A., & Hesser, J. E. 1974, ApJ, 192, 391
Hartwick, F. D. A., Hesser, J. E., & McClure, R. D. 1972, ApJ, 174, 557
Kassis, M., Janes, K. A., Friel, E. D., & Phelps, R. L. 1997, AJ, 113, 1723
King, I. R. 1962, AJ, 67, 471
King, I. R. 1966, AJ, 71, 64
Mayor, M. 1985, in IAU Coll. 88, ed. A. G. D. Philip, & D. W. Latham (New York: Schenectady, L. Davis Press), 35
Mayor, M., & Mermilliod, J.-C. 1984, Observational test of the stellar evolution theory, ed. A. Maeder, & A. Renzini (Dordrecht: Reidel), IAU Symp., 105, 411
Meibom, S., Andersen, J., & Nordström, B. 2002, A&A, 386, 187
Mermilliod, J.-C., & Mayor, M. 1992, in Binaries as tracers of stellar formation, ed. A. Duquennoy, & M. Mayor (Cambridge Univ. Press), 183
Mermilliod, J.-C., Huestamendia, G., del Rio, G., & Mayor, M. 1995, A&A, 307, 80
Mermilliod, J.-C., Clariá, J. J., Andersen, J., et al. 2001, A&A, 375, 30
Mermilliod, J.-C., Latham, D. W., Glushkova, E. V., et al. 2003, A&A, 399, 105
Momany, Y., Vandame, B., Zaggia, S., et al. 2001, A&A, 379, 436
Nordström, B., Andersen, J., & Andersen, M. I. 1997, A&A, 322, 460
Raboud, D., & Mermilliod, J.-C. 1994, A&A, 289, 121
Schwarzschild, M. 1954, AJ, 59, 273
Tinsley, B.-M., & King, I. R. 1976, AJ, 81, 835
Trumpler, R. J., & Weaver, H. F. 1962, Statistical Astronomy (New York: Dover Publications, Inc.), 121
Udry, S., Mayor, M., & Queloz, D. 1999, in Precise stellar radial velocities, IAU Colloq. 170, ed. J. B. Hearnshaw, & C. D. Scarfe, ASP Conf. Ser., 185, 367